Am J Physiol Endocrinol Metab 288: E71–E79, 2005.
First published August 31, 2004; doi:10.1152/ajpendo.00332.2004.

Respiratory uncoupling by UCP1 and UCP2 and superoxide generation in endothelial cell mitochondria

Brian D. Fink, Krzysztof J. Reszka, Judy A. Herlein, Mary M. Mathahs, and William I. Sivitz

Department of Internal Medicine, Division of Endocrinology and Metabolism, Iowa City Veterans Affairs Medical Center and the University of Iowa, Iowa City, Iowa

Submitted 26 July 2004; accepted in final form 21 August 2004

Fink, Brian D., Krzysztof J. Reszka, Judy A. Herlein, Mary M. Mathahs, and William I. Sivitz. Respiratory uncoupling by UCP1 and UCP2 and superoxide generation in endothelial cell mitochondria. *Am J Physiol Endocrinol Metab* 288: E71–E79, 2005. First published August 31, 2004; doi:10.1152/ajpendo.00332.2004.—Mitochondria represent a major source of reactive oxygen species (ROS), particularly during resting or state 4 respiration wherein ATP is not generated. One proposed role for respiratory mitochondrial uncoupling proteins (UCPs) is to decrease mitochondrial membrane potential and thereby protect cells from damage due to ROS. This work was designed to examine superoxide production during state 4 (no ATP production) and state 3 (active ATP synthesis) respiration and to determine whether uncoupling reduced the specific production of this radical species, whether this occurred in endothelial mitochondria per se, and whether this could be modulated by UCPs. Superoxide formation by isolated bovine aortic endothelial cell (BAE) mitochondria, determined using electron paramagnetic resonance spectroscopy, was approximately fourfold greater during state 4 compared with state 3 respiration. UCP1 and UCP2 overexpression both increased the proton conductance of endothelial cell mitochondria, as rigorously determined by the kinetic relationship of respiration to inner membrane potential. However, despite uncoupling, neither UCP1 nor UCP2 altered superoxide formation. Antimycin, known to increase mitochondrial superoxide, was studied as a positive control and markedly enhanced the superoxide spin adduct in our mitochondrial preparations, whereas the signal was markedly impaired by the powerful chemical uncoupler *p*-(trifluoromethoxyl)-phenyl-hydrazone. In summary, we show that UCPs do have uncoupling properties when expressed in BAE mitochondria but that uncoupling by UCP1 or UCP2 does not prevent acute substrate-driven endothelial cell superoxide as effluxed from mitochondria respiring in vitro.

endothelium; uncoupling protein; fatty acids; oxidative stress

MITOCHONDRIAL respiratory uncoupling is of considerable interest in vascular biology, since regulation of this process may play a protective role in atherogenesis, possibly through effects on reactive oxygen formation. Superoxide production, in particular, may be enhanced through substrate utilization and reduced by measures that decrease mitochondrial membrane potential (31). LDL receptor-deficient mice fed an atherosclerotic diet develop plaques. Lesion size and oxidative stress were greater when these mice were subject to bone marrow transplant derived from uncoupling protein (UCP)2(−/−) mice vs. UCP2(+/+) mice (2). Moreover, there is evidence for a role of UCP2 in the formation of reactive oxygen species (ROS) by endothelial cells per se. Mitochondrial membrane potential was enhanced in murine endothelial cells exposed to antisense oligonucleotides directed against UCP2 (9). This was associated with a rise in oxidative stress, assessed by thiobarbituric acid reactive substance (TBARS) values (9). In addition, UCPs may protect the endothelium from glycemic damage. Exposure of bovine aortic endothelial (BAE) cells to high glucose in the medium increased ROS detected by the fluorescence of chloromethyl-2′-7′-dichlorodihydrofluorescein (DCF) (24). This could be prevented by chemical uncoupling or overexpression of the brown adipose tissue protein UCP1.

Hence, UCPs may be important in modulating endothelial cell ROS. However, the above studies were limited, since TBARS and DCF fluorescence are not specific. Thus the nature of the oxidative stress and the particular ROS involved were not clear. In addition, more information is needed concerning the specific involvement of UCP2, the more ubiquitous UCP and the UCP subtype demonstrated to be present in endothelial cells (9). Information is also needed as to whether UCPs modulate ROS within mitochondria per se.

The current study was designed to determine whether uncoupling by UCPs alters superoxide generation by mitochondria of endothelial cells. We first determined whether UCPs in fact exhibit proton leak properties when expressed in mitochondria of BAE cells. Subsequently, we used electron paramagnetic resonance (EPR) spectroscopy to look specifically at the superoxide species and to address the issue of whether uncoupling by UCP1 and UCP2 modulated superoxide generation. We also examined the molar degree of expression of the UCPs in the mitochondria used to assess both the proton leak and the superoxide generation.

Uncoupling has been proposed as particularly important in protecting against ROS under "resting conditions," wherein ATP generation is not essential, thereby directing electron transport toward uncoupling or alternatively to work independent of ATP (3, 31). Hence, we were most interested in the effect of uncoupling BAE mitochondria on superoxide production during state 4 respiration (wherein ATP formation is prevented) as opposed to state 3 (active ATP synthesis). However, for comparison, and to determine whether superoxide production was actually less in these mitochondria during ATP generation, we also examined superoxide production and the effect of UCPs under state 3 conditions.

MATERIALS AND METHODS

Reagents and supplies. Adenoviral particles expressing full-length UCP2 and UCP1 and the oxoglutarate malate carrier (OMC) protein were grown and purified as previously described by our laboratory (12, 14). Affinity-purified polyclonal rabbit antibody directed against

Address for reprint requests and other correspondence: W. Sivitz, Dept. of Internal Medicine, Univ. of Iowa Health Care, 3E-17 VA, Iowa City, IA 52246 (E-mail: William-Sivitz@uiowa.edu).

The costs of publication of this article were defrayed in part by the payment of page charges. The article must therefore be hereby marked "*advertisement*" in accordance with 18 U.S.C. Section 1734 solely to indicate this fact.

UCP1, termed UCP12-A, was purchased from Alpha Diagnostics International (San Antonio, TX). Affinity-purified goat anti-UCP2 was purchased from Santa Cruz Biotechnology (Santa Cruz, CA). Antibody against OMC was obtained from rabbits immunized with two polypeptides prepared from conserved regions of OMC sequences (Arg^{48}–Ser^{64} and Asp^{156}–Gly^{175}) and characterized in previous studies (28, 29). Mouse anti-porin antibody (20B12) was purchased from Molecular Probes (Eugene, OR). Bovine erythrocyte superoxide dismutase (SOD) was purchased from Sigma (St. Louis, MO). Other reagents, kits, and supplies were as specified or purchased from standard sources.

Cell culture adenoviral infection. BAE cells were grown in medium M-199 (Invitrogen, Grand Island, NY) supplemented with MEM amino acids (Invitrogen), penicillin-streptomycin (Invitrogen), MEM vitamins (Sigma), and 20% fetal bovine serum (Hyclone, Logan, Utah) as described previously (21). Cells were grown to confluency in 150-cm^2 flasks between passages 6 and 12. For adenoviral expression, viral particles were applied at a titer of 3.1×10^6 pfu/cm^2 for 4 h in the absence of serum. The cells were then washed of virus, medium with 20% serum was added, and the cells were allowed to grow for 18 h.

Mitochondrial isolation. Cells were washed with PBS and scraped. Collected cells were homogenized using a Dounce homogenizer in ice-cold homogenization buffer (0.25 M sucrose, 5 mM HEPES, 0.1 mM EDTA, pH 7.2) with 0.1% fatty acid-free BSA. The homogenate was centrifuged at 500 *g* for 10 min. The pellet was discarded, and the supernatant was centrifuged again at 10,000 *g* for 10 min to obtain the mitochondrial pellet. The resulting pellet was then washed three times in homogenization buffer without BSA and resuspended in the respiration media described below. For immunoblotting, mitochondria were washed as above and homogenized by solubilization in detergent buffer (50 mM Tris, pH 7.2, 150 mM NaCl, 1% Triton X-100, 1% sodium deoxycholate, 0.1% SDS, and 2 mM EDTA). Protein was determined by the Bradford method (Bio-Rad, Hercules, CA).

Oxygen utilization and mitochondrial membrane potential. The rate of respiration of isolated mitochondria (0.2–0.4 mg protein/ml) was determined as previously described by our laboratory (12, 14). Concurrently, we assessed mitochondrial inner membrane potential based on the distribution (inside and external to the mitochondrial matrix) of the lipophilic cation tetraphenyl phosphonium (TPP^+) as we have previously described (12). To determine the concentration of TPP^+ inside the mitochondrial matrix, it is necessary to know the mitochondrial matrix volume and the extent to which TPP^+ is bound to mitochondrial protein as opposed to freely present within the matrix. Mitochondrial matrix volumes and the TPP^+ binding correction, under the conditions of incubation, were determined as previously carried out by our laboratory (12).

Determination of the proton leak. The proton leak was assessed as the kinetic relationship of H^+ flux to mitochondrial membrane potential through simultaneous recording of oxygen consumption and potential. Mitochondria were incubated in respiratory buffer [220 mM mannitol, 70 mM sucrose, 2.5 mM KH_2PO_4, 2 mM $MgCl_2$, 1 mM EDTA, 2 mM HEPES, pH 7.4, with 0.1% fatty acid-free BSA, 2 μM oligomycin to inhibit ATP synthase, 5 μM rotenone to inhibit electron entry at complex I, and 0.1 μM nigericin to abolish the ΔpH (20) across the mitochondrial membrane]. H^+ flux, under these conditions, is proton leak dependent and, with succinate as fuel, follows a 6:1 stoichiometry (H^+-O) with oxygen consumed (6, 7, 22, 26). Succinate (5 mM) was added, followed by malonate in incremental amounts to final concentrations of 0.05, 0.1, 0.2, 0.3, 0.4, 0.5, 1.0, and 2.0 mM to inhibit succinate dehydrogenase, thereby decreasing electrons available for the transport system and creating a range of membrane potentials (4).

Respiratory control ratio. Mitochondria were placed in respiratory buffer (minus oligomycin, nigericin, and rotenone) and incubated in the presence of excess succinate with limiting amounts of ADP as previously described by our laboratory (14). The respiratory control ratio (RCR) was calculated as the rate of oxygen consumption in the presence of ADP (state 3) divided by the rate in the absence of ADP (state 4).

Mitochondrial superoxide generation. EPR spectra were recorded using a Bruker EMX EPR spectrometer operating in X-band and equipped with a high-sensitivity resonator ER 4119HS. Samples were prepared at room temperature in 0.3 ml of respiratory buffer with 0.0688 M 5,5-dimethyl-L-pyrroline-*N*-oxide (DMPO) and 0.12 mg of isolated mitochondria. Substrate-induced respiration was initiated with the addition of succinate to a concentration of 6.67 mM, and samples were preincubated for 5 min in a 37°C water bath. Reactions were transferred to a flat aqueous EPR cell, and the spectra were recorded at room temperature with the following instrument settings: microwave power 40 mW, modulation amplitude 2 G, receiver gain 2×10^5, conversion time 40.96 ms, time constant 81.92 ms, and scan rate 80 G/41.92 s. Spectra shown are the average of 7–10 scans.

Fluorescent detection of mitochondrial ROS. ROS were also assessed as dihydroethidium (DHE) fluorescence. DHE is membrane permeate and, in the presence of superoxide, is oxidized to fluorescent ethidium, which is trapped by intercalation with DNA. Ethidium fluorescence was measured with the use of a BMG Fluostar Optima fluorescence spectrophotometer (BMG Labtechnologies, Durham, NC) at 37°C, with filter wavelengths of 544-nm absorbance and 620-nm emission. Samples were prepared in 96-well plates containing 0.06 ml/well of respiratory buffer with 20 μM DHE, 20 μg/ml of sheared salmon sperm DNA, and 6.67 mM succinate and mitochondria at a concentration of 0.05–0.1 mg/ml. Fluorescence in all wells was measured in relative units once every 65 s (1 cycle) and carried out for 65 cycles.

Immunoblotting. Mitochondrial protein was separated on 12.5% polyacrylamide gels, and immunoblotting was carried out as we have previously described (12, 14). We documented (12, 14) the specificity of the antibodies to UCP1 and UCP2 with competition by specific (but not by nonspecific) peptide to which these antibodies were raised, by demonstration of the appropriate tissue distribution of UCP1 or UCP2 immunoreactivity based on the reported mRNA distribution, and by demonstration of enhanced immunoreactivity in mitochondria compared with whole cell extracts and lack of cytoplasmic immunoreactivity.

Molar content of mitochondrial UCP1 and UCP2. To quantify UCP1 and UCP2 expression in BAE mitochondria, we engineered UCP1 and UCP2 proteins tagged with six histidine residues at the amino termini and expressed in *Escherichia coli* as we have previously described (12). Bacterial extracts were carefully quantified for protein by triplicate determination, using both the Bradford and Lowry techniques (which differed by <5%). The purity of these proteins was assessed on silver staining compared with a purified commercial preparation of G3PDH, and the absolute molar amounts of UCP1 and UCP2 were thus calculated. These inclusion body preparations were then employed as standards and run in multiple dilutions for quantitative immunoblotting to determine the molar content of UCP1 or UCP2 in the mitochondria employed in the electrochemical assessment of the kinetics of the proton leak and in the EPR experiments.

RESULTS

Mitochondrial volume (matrix space) and the TPP^+ binding correction were quantified in BAE mitochondria isolated from cells exposed to UCP1 ($n = 3$), UCP2 ($n = 3$), or no virus ($n = 4$). Respective volumes were (means ± SE) 2.63 ± 0.27, 2.56 ± 0.23, and 2.67 ± 0.39 μl/mg, and binding corrections (means ± SE) were 0.46 ± 0.02, 0.40 ± 0.05, and 0.39 ± 0.05. Because these parameters were very similar between groups and because they actually have minimal impact on calculated mitochondrial potential (due to the logarithmic re-

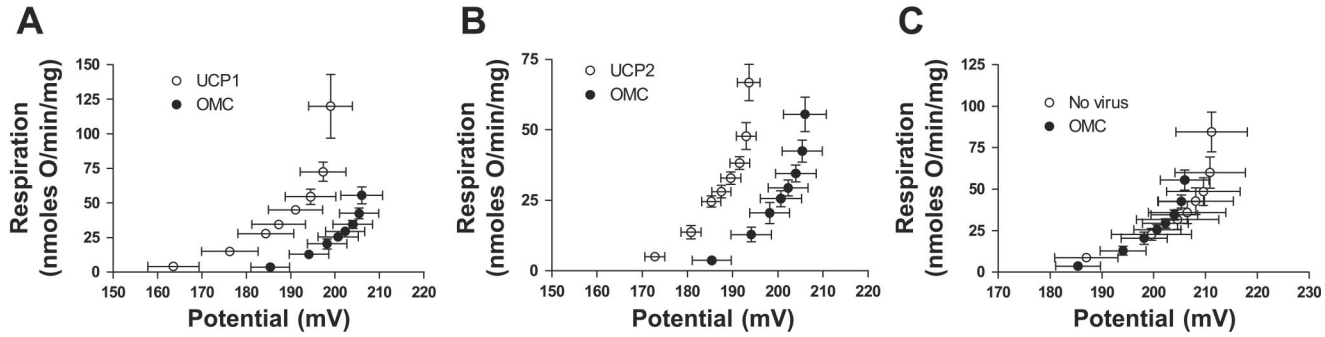

Fig. 1. Oxygen utilization as a function of inner membrane potential in mitochondria from bovine aortic endothelial cells (BAE) expressing adenoviral uncoupling protein (UCP)1 ($n = 5$) or oxoglutarate malate carrier (OMC) ($n = 7$) (*A*), UCP2 ($n = 8$) or OMC ($n = 7$) (*B*), or OMC ($n = 7$) or no virus ($n = 4$) (*C*). Incubations were carried out under state 4 conditions in respiratory buffer as described in MATERIALS AND METHODS. Succinate was added as fuel followed by incremental amounts of malonate to set membrane potential to a range of values. Data points represent means ± SE for both oxygen use and potential. The OMC data are reproduced in *A–C*, individually shown for clarity.

lationship of the Nernst equation), we assumed an overall average matrix space of 2.62 μl/mg of mitochondrial protein and a TPP^+ binding correction of 0.42. Moreover, any errors inherent in the isotopic methodology used to determine these parameters would cancel out in comparing groups exposed to different adenoviral conditions. We also applied these values to BAE mitochondria overexpressing the OMC protein, which, in our past studies of insulinoma mitochondria (12), did not affect matrix space or TPP^+ binding.

The RCR, averaged over four preparations, of BAE mitochondria unexposed to viral infection was 3.46 ± 0.79, a value comparable to that reported for several rat tissues and supportive of reasonably intact mitochondrial preparations (27). We also compared the RCR in BAE mitochondria exposed to the different adenoviral constructs. The mean RCR in mitochondria exposed to adenoviral OMC was 3.60 ± 0.38 (mean ± SE). As expected for uncoupling, the RCR values were reduced in mitochondria exposed to UCP1 or UCP2. These measured 2.80 ± 0.38 and 3.02 ± 0.60, respectively ($P < 0.05$ for UCP1 compared with OMC, $n = 4$ for each group, by one-way ANOVA).

As a better measure of respiratory uncoupling (5), we assessed the proton conductance of mitochondria isolated from BAE cells subject to adenoviral overexpression of UCP1, UCP2, or OMC or from BAE cells unexposed to viral particles. The results are depicted in Fig. 1, *A–C*. Data on the *y*-axis are proportional to proton flux, which, under the conditions of these experiments, is proportional to respiration with 6:1 stoichiometry (see MATERIALS AND METHODS). Thus proton conductance, as proton flux per unit potential, is defined at particular points on the curves.

Adenoviral infection with UCP1 or UCP2, compared with the control mitochondrial carrier protein OMC, shifted the curves (Fig. 1, *A* and *B*) upward and to the left, consistent with enhancement of the proton leak. Overexpression of the control protein OMC, compared with mitochondria from cells unexposed to viral particles, did not appreciably alter these kinetics (Fig. 1*C*). For statistical purposes, the data for individual experiments used to generate the curves of Fig. 1, *A* and *B*, were fit to second-order polynomial equations. The curve fits were use to compare respiration by mitochondria overexpressing UCP1, UCP2, or OMC at a membrane potential of 190 mV arbitrarily chosen as midrange. We also compared membrane potential at a respiratory rate of 35 nmol $O \cdot min^{-1} \cdot mg^{-1}$, likewise chosen as a midrange value. These analyses showed that both UCP1 and UCP2, compared with OMC, significantly reduced membrane potential (188 ± 5, 190 ± 2, and 200 ± 2 mV, respectively; $P < 0.05$ for UCP1 and UCP2 compared with OMC) and increased respiration (58 ± 18, 45 ± 10, and 12 ± 3 nmol $O \cdot min^{-1} \cdot mg^{-1}$, respectively; $P < 0.05$ for UCP1 and UCP2 compared with OMC) by one-way ANOVA.

To further assess the uncoupling action of UCP1 and UCP2 when overexpressed in BAE mitochondria, we examined the effect of GDP, a nucleotide felt to inhibit proton transfer by UCPs (11, 17, 23), on the proton leak kinetics of these mitochondria (Fig. 2, *A* and *B*). GDP inhibited the effect of UCP1 but not UCP2 on the proton conductance of BAE mitochondria. These effects were analyzed statistically as in the experiments of Fig. 1. In mitochondria overexpressing UCP1, GDP decreased respiration at an arbitrarily selected value of 195 mV (61.9 ± 15.7 in the absence of GDP vs. 14.2 ± 3.7 nmol $O \cdot min^{-1} \cdot mg\ protein^{-1}$ in the presence of

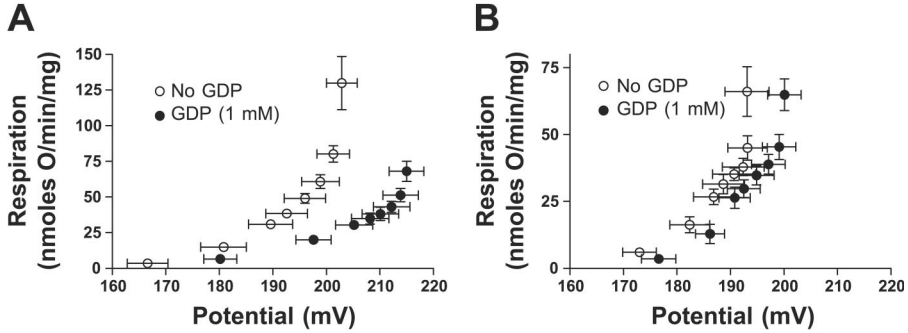

Fig. 2. Effect of GDP on proton conductance of mitochondria subject to overexpression of UCP1 or UCP2. Individual mitochondrial preparations were incubated in the presence or absence of GDP. *A*: UCP1, $n = 6$. *B*: UCP2, $n = 4$.

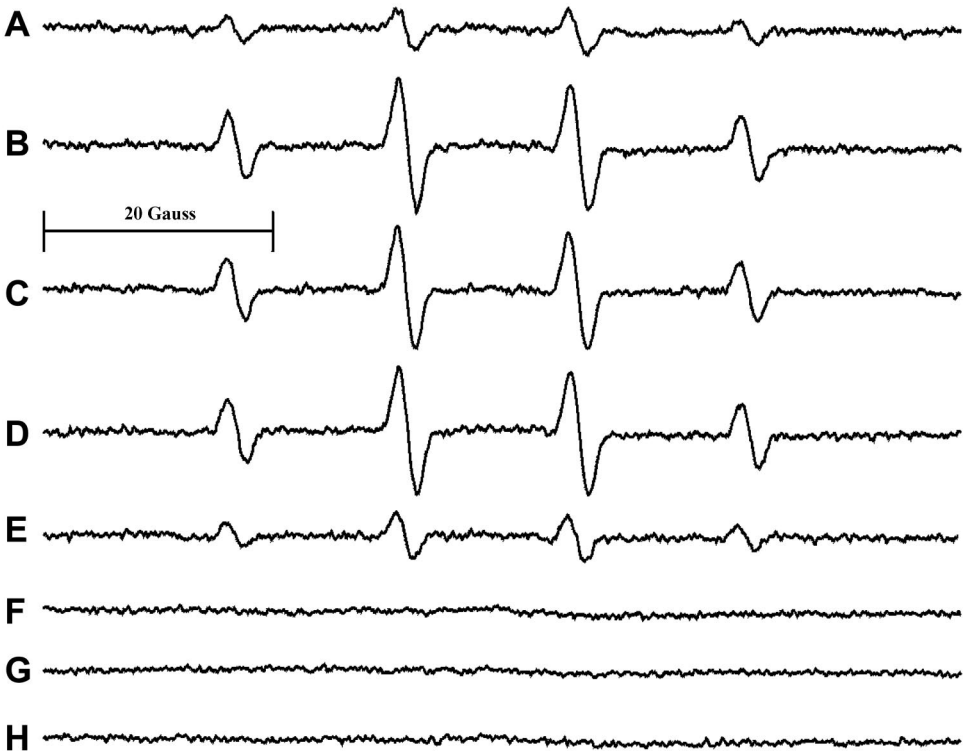

Fig. 3. Superoxide generation by BAE mitochondria incubated under state 4 conditions in respiratory buffer (see MATERIALS AND METHODS). Electron paramagnetic resonance (EPR) spectra were obtained from mitochondria subject to perturbations as follows. *A*: absence of succinate. *B*: no perturbation. *C*: UCP1 overexpression. *D*: UCP2 overexpression. *E*: addition of 2.5 μM *p*-(trifluoromethoxyl)-phenyl-hydrazone (FCCP). *F*: addition of superoxide dismutase (SOD; 300 U/ml). *G*: UCP1 overexpression plus addition of SOD (300 U/ml). *H*: UCP2 overexpression plus addition of SOD (300 U/ml).

GDP; $P < 0.05$ by paired *t*-test) and membrane potential at a respiratory rate of 50 nmol $O \cdot min^{-1} \cdot mg^{-1}$ (194.7 ± 3.6 in the absence of GDP vs. 213.0 ± 2.6 mV in the presence of GDP; $P < 0.01$ by paired *t*-test). In contrast, GDP had no significant effect on respiration or membrane potential when assessed in this way in mitochondria overexpressing UCP2.

In contrast to the relatively mild uncoupling by UCP1 and UCP2, addition of 2.5 μM *p*-(trifluoromethoxyl)-phenyl-hydrazone (FCCP) markedly reduced membrane potential to the point of abolishing net uptake of TPP^+ while increasing respiration (data not shown). This is the expected effect of this powerful chemical uncoupler (16).

Superoxide was quantitatively assessed by EPR spectroscopy as the decay product of the superoxide-DMPO adduct DMPO-OOH, which rapidly and spontaneously decays to the hydroxyl radical adduct DMPO-OH (36) (Figs. 3 and 4). The EPR spectra in Figs. 3 and 4 are those of DMPO-OH adducts, as determined on the basis of their characteristic splitting pattern (4 lines of intensity 1:2:2:1) and hyperfine splitting constants $a_N = 14.9$ G and $a_H^\beta = 14.9$ G. Thus the DMPO-OH spectra could possibly arise directly from the hydroxyl radical rather than the rapid decay of the superoxide adduct DMPO-OOH. However, control experiments showed that when SOD was present in the samples, the spectra were not observed (Figs. 3, *F–H*, and 4*C*), indicating that formation of DMPO-OH was entirely mediated by the superoxide radical.

Figures 3–5 depict superoxide production in BAE mitochondria exposed to various perturbations and incubated under state 4 conditions. As expected, succinate markedly increased superoxide generation compared with mitochondria examined in the absence of a fuel source. Superoxide production in the presence of succinate was diminished by the chemical uncoupler FCCP (Figs. 3 and 5*A*). In contrast to FCCP, superoxide generation was not affected by overexpression of either UCP1 or UCP2 (Figs. 3 and 5*B*). Antimycin, which is known to enhance superoxide formation through its effects on the Q cycle (30), markedly enhanced superoxide generation in the presence of succinate (Figs. 4 and 5*A*) and serves as a positive control. Moreover, adenoviral expression of UCP1 or UCP2 did not alter superoxide formation in the presence of antimycin (Fig. 5*C*).

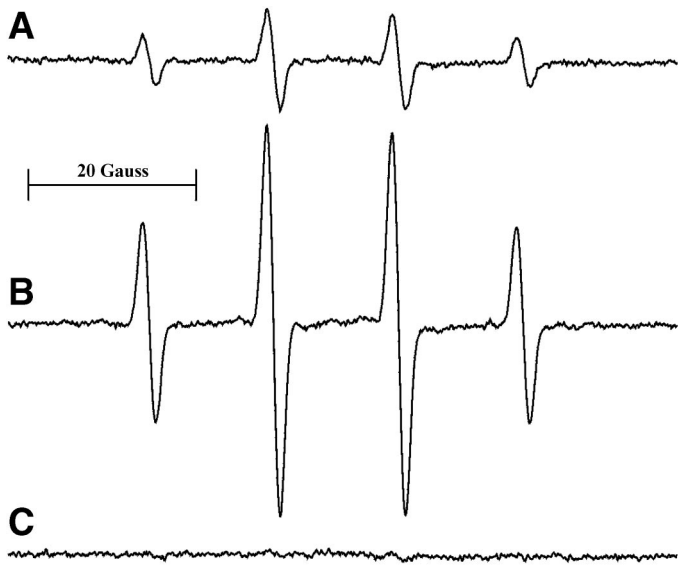

Fig. 4. Formation of superoxide by BAE mitochondria incubated in respiratory buffer as in Fig. 3 and subject to the following perturbations. *A*: no perturbation. *B*: addition of 10 μM antimycin. *C*: addition of 10 μM antimycin plus SOD (300 U/ml).

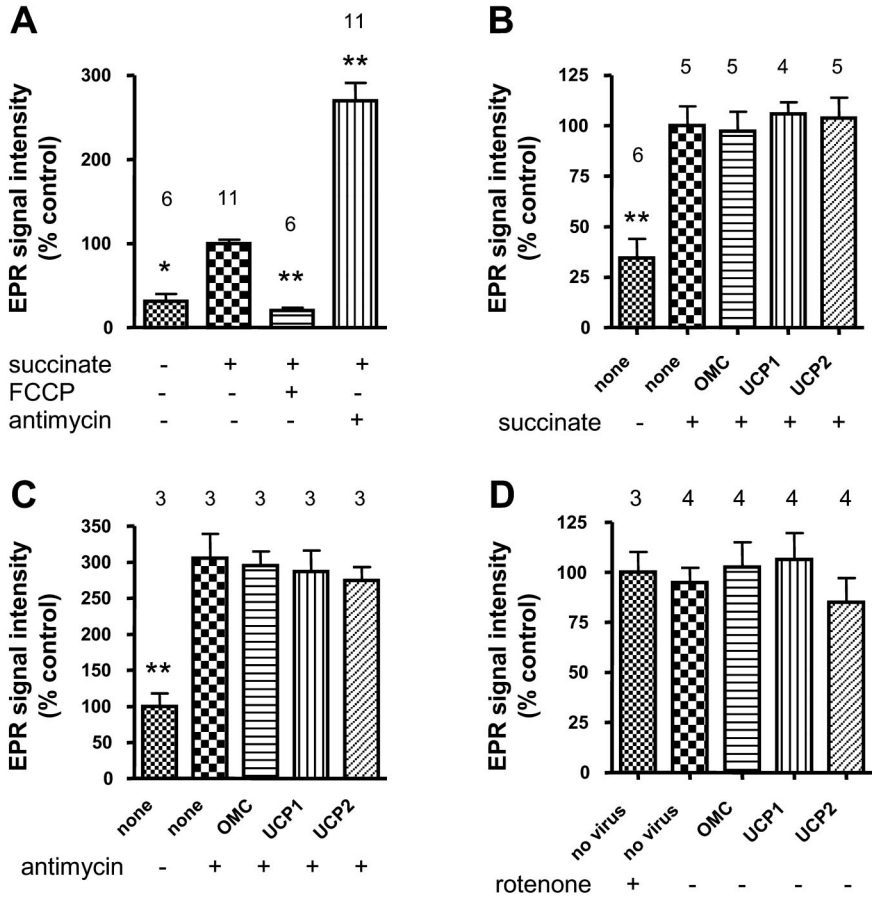

Fig. 5. Quantitative assessment of superoxide production by mitochondria isolated from BAE cells detected as in Figs. 3 and 4. Signal intensity was quantified as the integrated spectra. Mitochondria were incubated in respiratory buffer and perturbed as indicated. *A*: addition of 2.5 μM FCCP or 10 μM antimycin. *B*: mitochondria from BAE cells previously exposed to UCP1, UCP2, or OMC or with no adenoviral exposure (none). *C*: mitochondria exposed to adenoviral particles as in *B* and incubated in the presence of 6.7 mM succinate and 10 μM antimycin as indicated. *D*: repetition of experiments performed in *B* in the presence of succinate but the absence of rotenone except as shown. For each experiment, data were normalized to the mean intensity (arbitrarily defined as 100) of mitochondria unexposed to adenoviral particles incubated in the presence of succinate (control). $*P < 0.05$ or $**P < 0.01$ compared with control, by ANOVA with Dunnett post test; nos. above bars are *n*.

The complex I inhibitor rotenone was included in the above studies (Figs. 3–5, *A–C*). Respiration on succinate under these conditions should generate electron transport through ubiquinone to complex III, wherein the Q cycle would be the likely site for superoxide production. However, it has also been proposed that, in the absence of complex I inhibitors, respiration on succinate may generate reverse electron transport to this complex, another site strongly implicated in mitochondrial superoxide formation (34, 35). In this case, complex I should generate matrix superoxide, which may activate UCPs (34). Therefore, the experiments of Fig. 5*B* were repeated under the same conditions but in the absence of rotenone. As shown (Fig. 5*D*), the results were similar.

The specificity of the EPR signal for superoxide was verified by the addition of SOD to the incubation mixture. SOD abolished the EPR signal when added in the presence of succinate, whether in mitochondria overexpressing UCP1 or UCP2 or expressing no viral vector or in mitochondria exposed to antimycin (Figs. 3 and 4).

Figure 6*A* contrasts superoxide production under state 3 conditions to state 4. As shown, the magnitude of superoxide generation is markedly less during ATP production compared

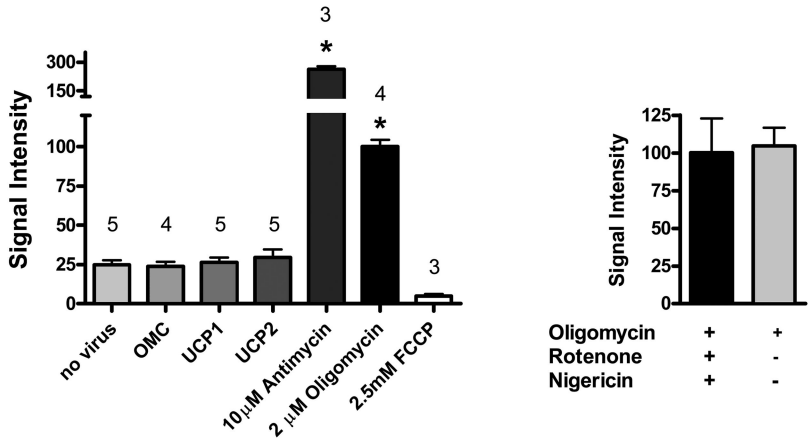

Fig. 6. *A*: quantitative assessment of superoxide production (detected as in Fig. 5) in mitochondria incubated in respiratory buffer (see MATERIALS AND METHODS) in the absence of oligomycin, nigericin, and rotenone and in the presence of excess (0.4 mM) ADP. Mitochondria were exposed to adenoviral particles as indicated or otherwise perturbed as shown. Hence, all incubations were carried out under state 3 conditions except for the group exposed to oligomycin to inhibit ATP synthase (state 4 respiration). For each experiment, the data were normalized to the mean intensity (arbitrarily defined as 100) of the group exposed to oligomycin. The absolute signal intensity of this group was approximately that of the control groups shown in Fig. 5. $*P < 0.01$ compared with OMC, by ANOVA with Dunnett posttest; nos. above bars are *n*. *B*: comparison of signal intensities between BAE mitochondria unexposed to adenoviral particles incubated in respiratory buffer in the presence or absence of rotenone plus nigericin ($n = 4$/group; P = not significant, by paired *t*-test).

with conditions wherein ATP synthesis is prevented (addition of oligomycin). We observed no detectable differences in state 3 superoxide generation between mitochondria exposed to no virus, OMC, UCP1, or UCP2. Antimycin did markedly enhance superoxide when incubated under state 3 conditions. The mitochondrial preparations of Fig. 5 were incubated in respiratory buffer that included rotenone and nigericin to assure that we examined superoxide production under the same conditions used to measure proton conductance (Fig. 1). However, rotenone and nigericin were not included in the incubations of Fig. 6*A*. Therefore, to better interpret the data of Figs. 5 and 6, we also examined superoxide production under state 4 conditions in the presence and absence of rotenone and nigericin. As shown in Fig. 6*B*, these agents did not alter superoxide formation.

We also examined the effect of UCP1 and UCP2 on mitochondrial ROS generation under state 4 conditions using a fluorescent technique. Although not necessarily specific for superoxide, DHE fluorescence was no different among mitochondria of BAE cells exposed to adenoviral UCP1, UCP2, or OMC or to no virus (means ± SE; 2.06 ± 0.17, 2.08 ± 0.19, 2.15 ± 0.20, and 2.10 ± 0.19 relative fluorescent units, respectively; $n = 9$ for each condition).

UCP1 and UCP2 expressions were quantified by comparing the immunoreactivity of the mitochondrial extracts used in our studies with the immunoreactivity of purified inclusion body preparations of UCP1 and UCP2. Silver staining (Fig. 7, *A* and *B*) revealed that these preparations were 64% (UCP2) and 9% (UCP1) pure. The validity of these numbers is supported by our previously reported studies (12) wherein we independently determined the histidine-tag immunoreactivity of these UCP2 and UCP1 preparations (12). The relative histidine-tag immunoreactivity for the UCP2 and UCP1 inclusion body preparations would be expected to be proportional to their relative molar content within these preparations or, in other words, their relative purity. We previously found that the histidine-tag immunoreactivity was seven- to eightfold greater for UCP2 compared with UCP1.

Figure 7*C* illustrates examples of the quantification of UCP1 and UCP2 in a portion of the mitochondrial preparations used in the studies described above of proton conductance or in our EPR studies of superoxide generation (see below). Figure 7*D* details the quantitative data over all these experiments and compares the molar degree of expression of UCP2 and UCP1. The data also show that the mean magnitudes of expression of UCP1 and of UCP2 did not differ between mitochondria utilized to examine proton conductance and those used in the studies of superoxide generation. Although we did not quantify the expression of the OMC protein in molar amounts, the immunoreactivity of this protein was increased at least 5- to 10-fold in mitochondria of BAE cells subject to adenoviral OMC compared with unexposed mitochondria, wherein the signal was quite weak (data not shown).

Finally, we examined the issue of the purity of the mitochondrial preparations used in these experiments. To address this, we measured the expression of porin, an abundant component of mitochondrial membranes. Porin expression remained reasonably constant among all mitochondrial preparations utilized. The coefficient of variation for porin expression among 53 different mitochondrial preparations examined was 9.9% and may be close to the accuracy of protein determination. There was also no difference in porin expression among mitochondria subject to adenoviral UCP1, UCP2, or OMC or to no virus.

DISCUSSION

Here we present novel data regarding the effects of respiratory uncoupling on superoxide formation by isolated mitochondria. We used rigorous methodology to specifically examine the superoxide radical and to characterize the effects of uncoupling agents on proton leak properties of these mitochondria.

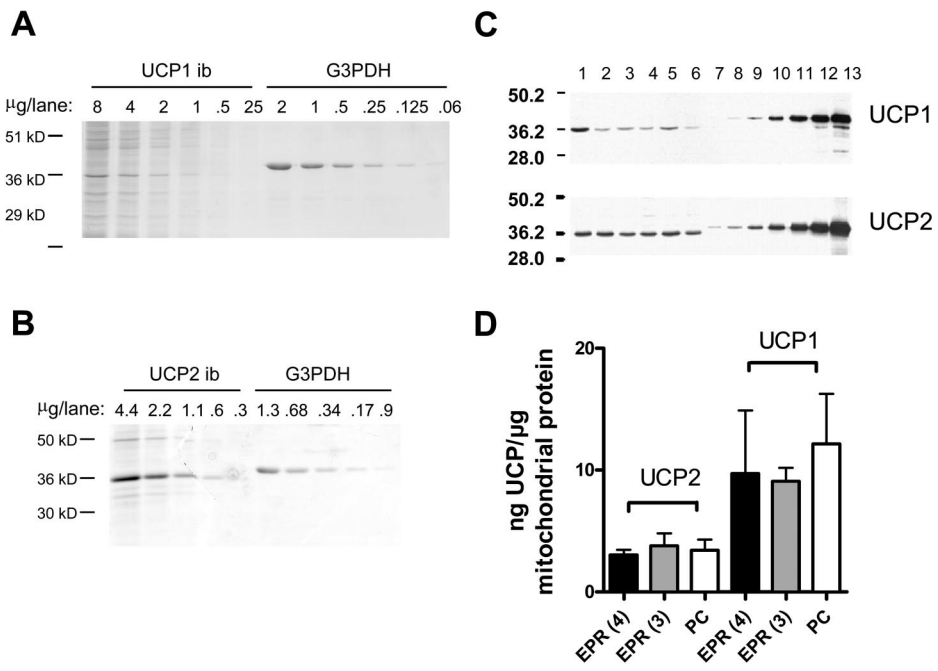

Fig. 7. Silver stains demonstrating the extent of purification of our histidine-UCP1 and histidine-UCP2 inclusion body (ib) preparations. *A*: histidine-UCP1 ib compared with a purified commercial preparation of G3PDH. *B*: histidine-UCP2 ib compared with G3PDH. If G3PDH is assumed 100% pure, then from plots of UCP1 ib or UCP2 ib densities vs. G3PDH densities (not shown), the UCP2 ib preparation is 64% pure and the UCP1 ib preparation is 9% pure. These nos. approximately agree with the relative histidine immunoreactivity of these histidine-tagged UCP1 and UCP2 preparations, which we determined independently (see RESULTS) and which reflect the relative (UCP2 vs. UCP1) molar UCP content. *C*: examples depicting UCP1 or UCP2 immunoreactivity by mitochondrial preparations overexpressing these proteins (*lanes 1–6* of each blot) compared with UCP1 or UCP2 ib preparations (*lanes 7–13*) consisting of serial 50% dilutions starting with 2,880 ng of UCP1 or 550 ng of UCP2 in the *right-most* lanes (*lane 13* of each blot). *D*: Mean (±SE) UCP1 and UCP2 expression in the mitochondrial preparations used in the proton conductance (PC) experiments of Fig. 1 and in the preparations used in subsequent EPR experiments (Figs. 5*B* and 6*A*) examining state 4 [EPR(4)] and state 3 [EPR(3)] respiration.

Because our intent was to examine the effect of UCPs on superoxide in mitochondria of endothelial cells, we felt it was very important to show that UCP1 and UCP2 do, in fact, uncouple respiration when expressed in mitochondria of these cells. The effect of UCP1 on proton leak kinetics (Fig. 1) was, as expected, consistent with the known effect of this protein to uncouple oxidative phosphorylation (23). This action of UCP1 was confirmed by the addition of GDP (Fig. 2*A*), a nucleotide known to inhibit UCP1-induced uncoupling. The kinetics for BAE mitochondria overexpressing UCP2 (Fig. 1) were likewise consistent with a role for UCP2 to uncouple, since H^+ flux was greater for any given potential. However, these kinetics, although blunted, were not significantly altered by GDP. These findings are similar to what was previously reported for UCP1 and UCP2 overexpression in mitochondria of insulinoma (INS-1) cells by our laboratory (12).

The level of endogenous expression of UCP2 within BAE cells is not clear, and we could not detect UCP2 in these cells by immunoblotting. However, the general experience is that available UCP2 antibodies lack sensitivity for most cells and tissues, although detecting higher levels in overexpressing mitochondria is not difficult (33). Furthermore, our antibody is directed at human and rodent UCP2, and reactivity with the bovine protein is questionable. Although the endogenous level of UCP2 expression in our BAE cells is not clear and UCP1 is presumably not expressed at all by BAE cells, the UCP concentrations in the mitochondria we examined are likely within or near the physiological range, at least for certain cell types. It has been estimated that spleen contains 0.313 μg of UCP2/mg of mitochondrial protein, and lung tissue exposed to lipopolysaccharide contains 2.9 times this amount (25, 33). If it is assumed that mitochondria of specific cell types within these tissues express even greater amounts, then the levels of UCP2 expressed in our BAE cells (Fig. 7) are likely comparable. Moreover, UCP1 in rodent brown adipose tissue mitochondria is actually present in higher levels (32), especially after acclimatization to cold, than in our BAE mitochondria overexpressing this protein.

Uncoupling may be an important means of protection from ROS. Manipulations that diminish mitochondrial potential decrease ROS formation. These include chemical uncouplers as well as ADP, phosphate, malonate (succinate dehydrogenase inhibition), and myxothiazol (18). Furthermore, fatty acids may induce a mild uncoupling and reduce ROS (31). A relation of UCP2 to ROS is suggested by studies of macrophages from UCP2 knockout mice. These animals generate more ROS than wild-type controls, and the mice show resistance to *Toxoplasma* infection reversible by quenching of ROS (1).

Hence, the major objective of the current work was to determine whether endothelial cell respiratory uncoupling by UCP modulates ROS generation, specifically superoxide and specifically within isolated mitochondria. Moreover, endothelial cells represent a cell type wherein ROS are of potential importance in the pathogenesis of atherosclerosis and vascular dysfunction (15).

Our results provide strong EPR evidence that superoxide represents at least one specific free radical species generated through substrate utilization by endothelial mitochondria. This follows, since the spin trap adduct depends on either superoxide or the hydroxyl radical, and the marked inhibition by SOD implicates the former particle. Our results (Fig. 6*A*) also show that superoxide is produced in substantially greater amounts by BAE mitochondria during "resting" or state 4 respiration, wherein ATP synthesis in prevented.

Generation of reactive oxygen by endothelial cells exposed to high mitochondrial nutrient flux has been proposed as a mechanism accounting for glycemic damage to the vasculature in diabetes mellitus. Nishikawa et al. (24) reported that incubating intact BAE cells at high media glucose concentration, which increased flux through the TCA cycle, enhanced ROS as DCF fluorescence. This effect of glucose was abolished by liposomal UCP1 overexpression as well as by chemical uncoupling, or by the mitochondrial-specific SOD (manganese SOD; MnSOD), suggesting a mitochondrial source.

Thus our current studies of isolated BAE mitochondria showing no effect of UCP1 or UCP2 may at first glance be discrepant with the above. However, there are factors that may explain this discrepancy. First, exposure of intact cells to glycemia to drive mitochondrial metabolism over hours to days is quite different from acute exposure of isolated mitochondria to succinate. In the first case, it is possible that changes in mitochondrial function or structure might be induced over time. Thus, when subsequently assessed for ROS, compared with cells exposed to physiological glycemia, the mitochondria could have acquired different characteristics. In fact, our results showing no effect of UCPs in isolated mitochondria support this contention. Thus chronic uncoupling by UCPs in cultured endothelial cells may have induced changes that manifest in the subsequent assessment of ROS. Yet we were unable to see differences due to UCPS in mitochondria acutely exposed to succinate. This reasoning may also explain why Nishikawa et al. (24) observed that MnSOD reduced DCF fluorescence. This observation has been appropriately questioned (13) based on the known action of MnSOD to convert superoxide to hydrogen peroxide, which should increase rather than decrease DCF fluorescence (which is most sensitive to hydrogen peroxide). However, if MnSOD had a chronic protective effect over the time of incubation, this could have prevented undefined superoxide-induced mitochondrial alterations that could manifest as increased ROS when DCF fluorescence was eventually determined. Another factor may be that our studies of UCPs in endothelial mitochondria used adenoviral expression of UCPs as opposed to liposomes (24). We documented expression in our studies, which was substantial, and it does not seem likely that greater expression was achieved with the liposomal technique.

It has been suggested that physiological reduction in mitochondrial potential through "mild uncoupling" may reduce superoxide formation, at least as generated through the Q cycle in complex 3. At this site, electron transport and generation of membrane potential under state 4 conditions would be expected to markedly enhance the formation and prolong the half-life of the one-electron reductant CoQ^-, which is highly reactive toward superoxide generation (30). Our data do show that uncoupling by FCCP reduced superoxide (Figs. 3 and 5) under state 4 conditions. FCCP was likely more effective than the UCPs simply because of the marked reduction in respiratory coupling associated with chemical transport of protons. In this regard, it has been shown that, below a certain threshold membrane potential, reactive oxygen is not generated (18), so FCCP essentially serves as a negative control (Fig. 5*A*) compared with the positive effect of antimycin. However, our data

do not support a role for UCPs as mild uncouplers protective from ROS.

We considered that UCPs might not have reduced superoxide formation because they were not activated to do so. In this regard, there is evidence that the effect of UCPs may be dependent on activation by superoxide from the matrix side of the mitochondrial membrane requiring CoQ as a cofactor (10, 11), although this is somewhat controversial (8). If this is the case, then the overexpressed UCPs in our experiments may not have been activated in the presence of succinate and rotenone, since generation of superoxide at complex I, needed for matrix activation of UCP, would not have occurred. However, in the absence of rotenone, succinate would be expected to induce reverse electron transport with consequent generation of superoxide at complex I. Hence, in the absence of rotenone, we reasoned that the UCPs now activated might reduced superoxide. However, this did not seem to be the case in our experiments, since our data were no different in the presence or absence of rotenone (Fig. 5). We acknowledge that there still may be a possibility that UCPs might only reduce matrix superoxide rather than superoxide that would exit the mitochondria. Our EPR studies should have only detected the latter, since superoxide was completely inhibited by added extramitochondrial MnSOD. In any case, our data clearly show that overexpressed UCPs do not reduce superoxide at complex III, which we readily detected based on the large increase in superoxide induced by antimycin.

In summary, we carried out rigid EPR assessment of superoxide effluxed from isolated mitochondria as affected by manipulations that uncouple endothelial cell respiration. Our data demonstrate *1*) specific production of the superoxide radical in isolated endothelial mitochondria respiring on succinate; *2*) that superoxide production was substantially enhanced under resting or state four conditions compared with state 3; and *3*) that overexpression of both UCP1 and UCP2 induced uncoupling properties in BAE mitochondria (however, neither protein reduced superoxide). These data suggest that uncoupling by UCP1 or UCP2 does not protect against superoxide effluxed from mitochondria or, alternatively, that the intact cellular environment is somehow necessary for this effect.

ACKNOWLEDGMENTS

EPR experiments were conducted in the EPR facility at the Iowa City Veterans Affairs Medical Center. We thank George T. Rasmussen for operating the EPR spectrometer.

GRANTS

This work was supported by the Department of Veterans Affairs Office of Research and Development and National Heart, Lung, and Blood Institute Grant RO1-HL-073166-01.

REFERENCES

1. **Arsenijevic D, Onuma H, Pecqueur C, Raimbault S, Manning BS, Miroux B, Couplan E, Alves-Guerra MC, Goubern M, Surwit R, Bouillaud F, Richard D, Collins S, and Ricquier D.** Disruption of the uncoupling protein-2 gene in mice reveals a role in immunity and reactive oxygen species production. *Nat Genet* 26: 435–439, 2000.
2. **Blanc J, Alves-Guerra MC, Esposito B, Rousset S, Gourdy P, Ricquier D, Tedgui A, Miroux B, and Mallat Z.** Protective role of uncoupling protein 2 in atherosclerosis. *Circulation* 107: 388–390, 2003.
3. **Boss O, Hagen T, and Lowell BB.** Uncoupling proteins 2 and 3: potential regulators of mitochondrial energy metabolism. *Diabetes* 49: 143–156, 2000.
4. **Brand MD.** The proton leak across the mitochondrial inner membrane. *Biochim Biophys Acta* 1018: 128–133, 1990.
5. **Brand MD, Brindle KM, Buckingham JA, Harper JA, Rolfe DF, and Stuart JA.** The significance and mechanism of mitochondrial proton conductance. *Int J Obes Relat Metab Disord* 23: S4–S11, 1999.
6. **Brown GC and Brand MD.** Proton/electron stoichiometry of mitochondrial complex I estimated from the equilibrium thermodynamic force ratio. *Biochem J* 252: 473–479, 1988.
7. **Chavin KD, Yang S, Lin HZ, Chatham J, Chacko VP, Hoek JB, Walajtys-Rode E, Rashid A, Chen CH, Huang CC, Wu TC, Lane MD, and Diehl AM.** Obesity induces expression of uncoupling protein-2 in hepatocytes and promotes liver ATP depletion. *J Biol Chem* 274: 5692–5700, 1999.
8. **Couplan E, del Mar Gonzalez-Barroso M, Alves-Guerra MC, Ricquier D, Goubern M, and Bouillaud F.** No evidence for a basal, retinoic, or superoxide-induced uncoupling activity of the uncoupling protein 2 present in spleen or lung mitochondria. *J Biol Chem* 277: 26268–26275, 2002.
9. **Duval C, Negre-Salvayre A, Dogilo A, Salvayre R, Penicaud L, and Casteilla L.** Increased reactive oxygen species production with antisense oligonucleotides directed against uncoupling protein 2 in murine endothelial cells. *Biochem Cell Biol* 80: 757–764, 2002.
10. **Echtay KS, Murphy MP, Smith RA, Talbot DA, and Brand MD.** Superoxide activates mitochondrial uncoupling protein 2 from the matrix side. Studies using targeted antioxidants. *J Biol Chem* 277: 47129–47135, 2002.
11. **Echtay KS, Roussel D, St-Pierre J, Jekabsons MB, Cadenas S, Stuart JA, Harper JA, Roebuck SJ, Morrison A, Pickering S, Clapham JC, and Brand MD.** Superoxide activates mitochondrial uncoupling proteins. *Nature* 415: 96–99, 2002.
12. **Fink BD, Hong YS, Mathahs MM, Scholz TD, Dillon JS, and Sivitz WI.** UCP2-dependent proton leak in isolated mammalian mitochondria. *J Biol Chem* 277: 3918–3925, 2002.
13. **Green K, Brand MD, and Murphy MP.** Prevention of mitochondrial oxidative damage as a therapeutic strategy in diabetes. *Diabetes* 53: S110–S118, 2004.
14. **Hong Y, Fink BD, Dillon JS, and Sivitz WI.** Effects of adenoviral overexpression of uncoupling protein-2 and -3 on mitochondrial respiration in insulinoma cells. *Endocrinology* 142: 249–256, 2001.
15. **Irani K.** Oxidant signaling in vascular cell growth, death, and survival : a review of the roles of reactive oxygen species in smooth muscle and endothelial cell mitogenic and apoptotic signaling. *Circ Res* 87: 179–183, 2000.
16. **Kadenbach B.** Intrinsic and extrinsic uncoupling of oxidative phosphorylation. *Biochim Biophys Acta* 1604: 77–94, 2003.
17. **Klingenberg M, Echtay KS, Bienengraeber M, Winkler E, and Huang SG.** Structure-function relationship in UCP1. *Int J Obes Relat Metab Disord* 23, *Suppl* 6: S24–S29, 1999.
18. **Korshunov SS, Skulachev VP, and Starkov AA.** High protonic potential actuates a mechanism of production of reactive oxygen species in mitochondria. *FEBS Lett* 416: 15–18, 1997.
19. **Lionetti L, Iossa S, Liverini G, and Brand MD.** Changes in the hepatic mitochondrial respiratory system in the transition from weaning to adulthood in rats. *Arch Biochem Biophys* 352: 240–246, 1998.
20. **Moser DR, Lowe WL Jr, Dake BL, Booth BA, Boes M, Clemmons DR, and Bar RS.** Endothelial cells express insulin-like growth factor-binding proteins 2 to 6. *Mol Endocrinol* 6: 1805–1814, 1992.
21. **Nicholls DG.** The non-Ohmic proton leak—25 years on. *Biosci Rep* 17: 251–257, 1997.
22. **Nicholls DG and Locke RM.** Thermogenic mechanisms in brown fat. *Physiol Rev* 64: 1–64, 1984.
23. **Nishikawa T, Edelstein D, Du XL, Yamagishi S, Matsumura T, Kaneda Y, Yorek MA, Beebe D, Oates PJ, Hammes HP, Giardino I, and Brownlee M.** Normalizing mitochondrial superoxide production blocks three pathways of hyperglycaemic damage. *Nature* 404: 787–790, 2000.
24. **Pecqueur C, Alves-Guerra MC, Gelly C, Levi-Meyrueis C, Couplan E, Collins S, Ricquier D, Bouillaud F, and Miroux B.** Uncoupling protein 2, in vivo distribution, induction upon oxidative stress, and evidence for translational regulation. *J Biol Chem* 276: 8705–8712, 2001.
25. **Porter RK, Joyce OJ, Farmer MK, Heneghan R, Tipton KF, Andrews JF, McBennett SM, Lund MD, Jensen CH, and Melia HP.** Indirect

measurement of mitochondrial proton leak and its application. *Int J Obes Relat Metab Disord* 23, *Suppl* 6: S12–S18, 1999.
27. **Rolfe DF, Hulbert AJ, and Brand MD.** Characteristics of mitochondrial proton leak and control of oxidative phosphorylation in the major oxygen-consuming tissues of the rat. *Biochim Biophys Acta* 1188: 405–416, 1994.
28. **Scholz TD, Koppenhafer SL, tenEyck CJ, and Schutte BC.** Ontogeny of malate-aspartate shuttle capacity and gene expression in cardiac mitochondria. *Am J Physiol Cell Physiol* 274: C780–C788, 1998.
29. **Scholz TD, TenEyck CJ, and Schutte BC.** Thyroid hormone regulation of the NADH shuttles in liver and cardiac mitochondria. *J Mol Cell Cardiol* 32: 1–10, 2000.
30. **Skulachev VP.** Role of uncoupled and non-coupled oxidations in maintenance of safely low levels of oxygen and its one-electron reductants. *Q Rev Biophys* 29: 169–202, 1996.
31. **Skulachev VP.** Uncoupling: new approaches to an old problem of bioenergetics. *Biochim Biophys Acta* 1363: 100–124, 1998.
32. **Stuart JA, Harper JA, Brindle KM, Jekabsons MB, and Brand MD.** A mitochondrial uncoupling artifact can be caused by expression of uncoupling protein 1 in yeast. *Biochem J* 356: 779–789, 2001.
33. **Stuart JA, Harper JA, Brindle KM, Jekabsons MB, and Brand MD.** Physiological levels of mammalian uncoupling protein 2 do not uncouple yeast mitochondria. *J Biol Chem* 276: 18633–18639, 2001.
34. **Talbot DA, Lambert AJ, and Brand MD.** Production of endogenous matrix superoxide from mitochondrial complex I leads to activation of uncoupling protein 3. *FEBS Lett* 556: 111–115, 2004.
35. **Votyakova TV and Reynolds IJ.** DeltaPsi(m)-Dependent and -independent production of reactive oxygen species by rat brain mitochondria. *J Neurochem* 79: 266–277, 2001.
36. **Zwicker K, Dikalov S, Matuschka S, Mainka L, Hofmann M, Khramtsov V, and Zimmer G.** Oxygen radical generation and enzymatic properties of mitochondria in hypoxia/reoxygenation. *Arzneimittelforschung* 48: 629–636, 1998.